Title

SHP2 inhibition enhances the effects of tyrosine kinase inhibitors in preclinical models of treatment-naïve *ALK-*, *ROS1-*, or *EGFR*-altered non-small-cell lung cancer

Author's name and affiliation

Hirohisa Kano[1)], Eiki Ichihara[2)], Hiromi Watanabe[1)], Kazuya Nishii[1)], Chihiro Ando[1)], Takamasa Nakasuka[1)], Kiichiro Ninomiya[1)], Yuka Kato[3)], Toshio Kubo[4)], Kammei Rai[2)], Kadoaki Ohashi[2)], Katsuyuki Hotta[3)], Masahiro Tabata[4)], Yoshinobu Maeda[1)] and Katsuyuki Kiura[2)]

1) Department of Hematology, Oncology and Respiratory Medicine, Okayama University Graduate School of Medicine, Dentistry, and Pharmaceutical Sciences, Japan

2) Department of Allergy and Respiratory Medicine, Okayama University Hospital, Japan

3) Center for Innovative Clinical Medicine, Okayama University Hospital, Japan

4) Cancer Center, Okayama University Hospital, Japan

Running Title

Oncogene targeted therapy combined with SHP2 inhibitor in NSCLCs

Corresponding author:

Eiki Ichihara, MD, PhD

Okayama University Hospital, Okayama, Japan (Country code +81).

2-5-1 Shikata-cho Kita-ku Okayama City, Okayama 700-8558, Japan,

Tel.: +81-86-235-7227 E-mail: ichiha-e@md.okayama-u.ac.jp

Financial Information

This work was supported by grants from Project Mirai, the Ryobi Teien Memory Foundation, the Okayama Medical Foundation and the Japan Lung Cancer Society.

Abstract

After molecular-targeted therapy, some cancer cells may remain that are resistant to therapies targeting oncogene alterations, such as those in the genes encoding the epidermal growth factor receptor (*EGFR*) and anaplastic lymphoma kinase (*ALK*) as well as c-ros oncogene 1 (*ROS1*). The mechanisms underlying this type of resistance are unknown. Here we report the potential role of Src homology 2 domain-containing phosphatase 2 (SHP2) in the residual cells of *ALK*/*ROS1*/*EGFR*-altered non-small-cell lung cancer (NSCLC). Molecular-targeted therapies failed to inhibit the ERK signaling pathway in the residual cells whereas the SHP2 inhibitor SHP099 abolished their remaining ERK activity. SHP099 administered in combination with molecular-targeted therapy resulted in marked growth inhibition of cancer cells both *in vitro* and *in vivo*. Thus, treatment combining an SHP2 inhibitor and a tyrosine kinase inhibitor may be a promising therapeutic strategy for oncogene-driven NSCLC.

Introduction

Agents targeting gene mutations/translocations in oncogenes, such as the genes encoding epidermal growth factor receptor (*EGFR*) and anaplastic lymphoma kinase (*ALK*) as well as c-ros oncogene 1 (*ROS1*), remarkably inhibit the growth of non-small-cell lung cancer (NSCLC) (1-6). However, there is often residual tumor after these therapies, leading to acquired resistance and poor curative efficacy (7-11). Despite efforts to develop post-resistance therapies to overcome acquired resistance (12-16), most therapies do not work well due to the diversity of resistance mechanisms, difficulty of re-biopsy, and emergence of further resistance.

It is unclear why residual tumor remains after strong inhibition of oncogenic signaling. A possible mechanism is that downstream signaling inhibited by the molecular agent is somehow compensated. This was demonstrated in an *EGFR*-mutant NSCLC, in which treatment with the third-generation EGFR tyrosine kinase inhibitor (TKI) osimertinib induced reactivation of extracellular signal-regulated kinase (ERK) following transient ERK inhibition (17). Combination therapy consisting of a mitogen-activated protein kinase (MAPK)/ERK kinase (MEK) inhibitor and an EGFR TKI inhibited this reactivation and had a profound inhibitory effect on the cancer cells (18), suggesting its potential therapeutic efficacy in *EGFR*-mutant lung cancer (19).

Src homology 2 domain-containing phosphatase 2 (SHP2), a tyrosine phosphatase encoded by *protein-tyrosine phosphatase non-receptor type 11* (*PTPN11*), mediates cell signaling from multiple receptor tyrosine kinases (RTKs) to their downstream pathways, including the MAPK pathway. Germline PTPN11 gene mutations are frequently found in Noonan syndrome (20), which is characterized by congenital malformations. Somatic PTPN11 gene mutations have also been implicated in cancers such as juvenile myelomonocytic leukemia (21), hepatocellular carcinoma (22), acute myeloid leukemia (23), colorectal cancer (24), breast cancer (25), melanoma (26) and lung cancer (27, 28). Recently developed allosteric SHP2 inhibitors such as SHP099 and RMC-4550 have been shown to be highly effective, especially in RAS/RAF/MAPK-pathway-driven cancers such as *BRAF* mutant melanoma (29-33). In addition, in an RTK-driven NSCLC, an SHP2 inhibitor restored sensitivity to the ALK TKI ceritinib in *ALK*-rearranged NSCLC cells that had acquired resistance to the drug (34). However, only a few studies have examined the use of an SHP2 inhibitor combined with an RTK inhibitor in a model of treatment-naïve RTK driven NSCLC (35-37). These include two reports of the efficacy of SHP2 inhibitor combined with an RTK inhibitor in *EGFR*-mutant NSCLC cell lines (36, 37), but there are no data regarding *ALK/ROS1* rearranged NSCLC. Thus, in this study, we evaluated the efficacy

of the SHP2 inhibitor SHP099 against residual tumor cells following molecular-targeted therapy in a model of treatment-naïve *ALK*/*ROS1*/*EGFR*-altered NSCLC.

Materials and Methods

Cell lines and reagents

PC-9 cells (*EGFR* Ex19 del E746_A750) were purchased from the European Collection of Authenticated Cell Cultures (Salisbury, UK). HCC827 (*EGFR* Ex19 del E746_A750), H3122 (EML4-ALK fusion), and HCC78 (SLC34A2-ROS1 fusion) cells were kindly provided by Dr. William Pao (Vanderbilt University, Nashville, TN, USA). ABC-19 (EML4-ALK fusion) and ABC-20 (CD74-ROS1 fusion) cells were obtained from NSCLC patients and established as cell lines in our laboratory (38). All cell lines were cultured in RPMI-1640 medium (Sigma-Aldrich, St. Louis, MO, USA) supplemented with 10% heat-inactivated fetal bovine serum and 1% penicillin/streptomycin and were maintained at 37°C in a 5% CO_2 humified atmosphere. Alectinib, crizotinib, osimertinib, SHP099, selumetinib, RMC-4550 and DS-6051b were purchased from Selleck Chemicals (Houston, TX, USA). All compounds were dissolved in dimethyl sulfoxide for *in vitro* studies.

Cell imaging and cell proliferation assay

The cells were seeded in a 10-cm dish (PC-9: 250,000 cells/dish; H3122 and HCC78: 1,000,000 cells/dish) and treated the following day. After 48 h, cell mass and

morphology were observed under an inverted phase-contrast microscope, and images were obtained. Growth inhibition was measured in a modified 3-(4,5-dimethylthiazol-2-yl)-2,5-diphenyltetrazolium bromide (MTT) assay (39). Briefly, the cells were seeded in 96-well plates at a density of 1,500–10,000 cells/well (PC-9: 1,500 cells/well; H3122, HCC78, HCC827: 3,000 cells/well; ABC-19: 4,000 cells/well; ABC-20: 10,000 cells/well) and continuously treated with each drug for 96 h.

Crystal violet assay

The cells were seeded in six-well plates at a density of 10,000–600,000 cells/well (H3122: 600,000 cells/well; ABC19: 80,000 cells/well; HCC78: 20,000 cells/well; ABC-20: 200,000 cells/well; PC-9: 10,000 cells/well; HCC827: 20,000 cells/well) and treated the following day. Media and drugs were replaced 3 days after the first treatment. After fixation in 10% formalin for 10 min, the cells were stained for 10 min with crystal violet solution (Sigma-Aldrich) and then washed with H_2O. The plates were dried overnight and the stained cells were then quantified using ImageJ software (version 1.52a; National Institutes of Health, Bethesda, MD, USA).

Combination index (CI)

A constant ratio design for the combination assay was used because it enables efficient data analysis (40). The multiple-drug-effect analysis, developed by Chou and Talaly, is based on the median-effect principle and was used in this study to calculate the combined drug effect (41). Cells seeded in triplicate in 96-well plates were treated for 96 h with TKIs and/or SHP099 at the indicated concentrations. Cell viability was assessed using the MTT assay. The CIs were calculated using CompuSyn software (CompuSyn, Paramus, NJ, USA), developed by Chou *et al*. in 2010 (42). In the plots generated by CompuSyn, the y-axis represents the CI, with CI < 1, 1 or > 1 indicating a synergistic, additive or antagonistic effect respectively. The x-axis represents the fractional activity (Fa), which is the proportion of cells inhibited by the treatment relative to that inhibited by the vehicle control.

Immunoblotting and RTK array

Immunoblotting was conducted using the following antibodies: phosphorylated (p)-ALK Tyr1282/1283 (#9687), ALK (#3633), p-ROS1 Tyr2274 (#3078), ROS1 (#3287), p-EGFR Tyr1068 (#3777), EGFR (#2232), SHP2 (#3752), p-MEK1/2 Ser217/221 (#9154), MEK1/2 (#9126), p-ERK1/2 Thr202/Tyr204 (#9101), ERK1/2 (#9102), p-AKT Ser473 (#9271), AKT (#9272), and GAPDH (#2118), obtained from

Cell Signaling Technology (Danvers, MA, USA), and anti-SHP2 (phosphor Y542) antibody (ab62322), obtained from Abcam (Cambridge, MA, USA). Anti-rabbit IgG horseradish peroxidase-linked whole antibody (from donkey; NA934) was purchased from GE Healthcare Biosciences (Pittsburgh, PA, USA). For immunoblotting, the harvested cells were washed in phosphate-buffered saline and lysed in radioimmunoprecipitation assay buffer (1% IGEPAL CA-630 [MP Biochemicals, Irvine, CA, USA], 0.1% sodium dodecyl sulphate, 1% okadaic acid, 50 mM Tris-HCl, pH 7.5, 75 mM NaCl, 40 mM NaF and 1 mM sodium orthovanadate) containing a protease inhibitor cocktail (Roche Applied Sciences, Penzberg, Germany). The proteins were separated by SDS-PAGE and then electrotransferred onto membranes, which were then incubated with the indicated primary and secondary antibodies. Chemiluminescence was performed using Enhanced Chemiluminescence Plus reagent (GE Healthcare Biosciences, Chicago, IL, USA). Bands were detected using an ImageQuant LAS-4000 imager (GE Healthcare Biosciences) and quantified using ImageJ software (version 1.52a). A Phospho-RTK Array Kit was purchased from R&D Systems and used according to the manufacturer's recommendations.

Xenograft mouse models

Female BALB/c nu/nu mice (6 weeks old) were purchased from Charles River

Laboratories, Yokohama, Japan). All mice were provided with sterilized food and water and housed in a barrier facility under a 12-h light/dark cycle. Cancer cells (H3122, PC-9: 2×10^6 cells/tumor; ABC-20: 4×10^6 cells/tumor) were injected subcutaneously into the backs of the mice on the right and left sides. For combination treatment with SHP099 and TKI, when the average tumor volume reached ~200 mm^3, the mice were randomly allocated into four treatment groups (five mice/group): vehicle, SHP099 (50 mg/kg/day), TKI (alectinib, 10 mg/kg/day; crizotinib, 50 mg/kg/day; osimertinib, 5 mg/kg/day), and SHP099 plus TKI. Both SHP099 and the TKI were administered by gavage once daily, five times weekly. Tumor volume ($width^2 \times length/2$) was measured periodically. Statistical analyses were conducted based on the tumor volume measured on day 28. For comparison of SHP099 and selumetinib in combination with osimertinib, when the average tumor volume reached ~200 mm^3, the mice were randomly allocated into three treatment groups (five mice/group): osimertinib (5 mg/kg/day), selumetinib (50 mg/kg/day) plus osimertinib, and SHP099 (50 mg/kg/day) plus osimertinib. Osimertinib, selumetinib and SHP099 were administered by gavage once daily, five times weekly. Tumor volume ($width^2 \times length/2$) was measured periodically. Statistical analyses were conducted based on the tumor volume measured on day 14. All experiments involving animals were performed under the auspices of the Institutional

Animal Care and Research Advisory Committee at the Department of Animal Resources, Okayama University Advanced Science Research Center (Okayama, Japan). The experiments were performed under the Policy on the Care and Use of Laboratory Animals, Okayama University, and Fundamental Guidelines for Proper Conduct of Animal Experiment and Related Activities in Academic Research Institutions, Ministry of Education, Culture, Sports, Science and Technology of Japan. The experimental protocol was approved by the Animal Care and Use Committee of Okayama University (OKU-2019521).

Statistical analysis

The statistical analyses were performed using STATA software (version 15; StataCorp, College Station, TX, USA). Differences between two groups were compared using the two-tailed paired Student's *t*-test, and differences among three groups were compared in a one-way analysis of variance (ANOVA) followed by the Bonferroni method. A P value < 0.05 was considered to indicate statistical significance.

Results

Characterization of residual *ALK*/*ROS1*/*EGFR*-altered NSCLC cells after molecular-targeted therapy

To investigate whether TKI tolerance in the clinical setting could be simulated in a preclinical model, *ALK*/*ROS1*/*EGFR*-altered NSCLC cells were treated with the following drugs: alectinib for *ALK*-rearranged cells, crizotinib for *ROS1*-rearranged cells and osimertinib for *EGFR*-mutant cells. Each agent effectively inhibited the majority of the cancer cells, but in each case some cells remained even after 48 h of drug exposure (Fig. 1A). The cell signaling status in the residual cells was determined by treating each cell line as described followed by immune blotting at different time points thereafter. After 4 h of treatment, phosphorylation of the following driver oncogenes was effectively inhibited (Fig. 1B). In *ALK*-rearranged NSCLC cells (H3122 and ABC-19), ALK-TKI alectinib completely inhibited ALK phosphorylation over the studied period, whereas ERK activity was partially sustained or reactivated despite treatment with the inhibitor for 24 and 72 h (Fig. 1B, left). ERK phosphorylation was investigated in *ROS1*-rearranged or *EGFR*-mutant NSCLC cells. In the former (HCC78 and ABC-20), treatment with the ROS1-TKI crizotinib completely inhibited ROS1 phosphorylation, whereas ERK phosphorylation was partially reactivated without upstream ROS1 activation (Fig. 1B, center). ERK phosphorylation was also partially

sustained or reactivated over time in *EGFR*-mutant cells (PC-9 and HCC827) treated with the EGFR-TKI osimertinib, whereas EGFR phosphorylation was completely inhibited (Fig. 1B, right). These results demonstrate the persistent activity of the ERK pathway after TKI exposure in all of the examined cell lines and imply that a sustained ERK pathway plays a role in the resistance of NSCLC treated with TKIs. In the experiment focusing on the AKT pathway, while in some cells phosphorylated AKT was completely inhibited, in others it was not (Fig. 1B).

An SHP2 inhibitor suppresses sustained ERK and AKT phosphorylation in the presence of TKI

We hypothesized a role for another RTK in sustaining or reactivating the ERK pathway in the residual tumor cells after TKI exposure. However, a search using a phosphorylated RTK array showed simultaneous and slight activation of various bypass RTKs following TKI treatment, with none of them targeted by a single agent (Supplementary Fig. 1). Thus, to control this broadly activated signaling in the residual cells, we focused on SHP2 as a common targetable node of multiple RTK signaling, given that this phosphatase serves as an important hub that mediates RTK signaling to the downstream ERK pathway.

First, the efficacy of the SHP2 inhibitor SHP099 on oncogene activation in residual cells under TKI therapy was tested. *ALK*- or *ROS1*-rearranged cells as well as *EGFR*-mutant cells were treated for 24 h with the corresponding TKI with or without SHP099, after which signal activation was evaluated (Fig. 2). Alectinib with or without SHP099 completely inhibited p-ALK in *ALK*-rearranged NSCLC cells (H3122 and ABC19). Although alectinib or SHP099 alone did not completely suppress ERK and its upstream activation of MEK, both proteins were strongly suppressed by a combination of the two drugs (Fig. 2, left). In *ROS1*-rearranged cells (HCC78 and ABC-20), p-ROS1 levels were strongly suppressed by crizotinib, but whereas crizotinib or SHP099 treatment alone had a partial effect on p-MEK and p-ERK, their combined use resulted in strong suppression of the proteins (Fig. 2, center). Because crizotinib is a multi-targeting agent that inhibits ROS1, ALK and MET, the efficacy of another ROS1 TKI, DS-6051b (16), was investigated in combination with SHP099 in *ROS1*-rearranged HCC78 and ABC-20 cells (Supplementary Fig. 2A). Consistent with the effect of crizotinib, greater inhibition of p-ERK was obtained with DS-6051b in combination with SHP099 than with DS-6051b alone. Similarly, in *EGFR*-mutant NSCLC cells (PC-9 and HCC827), combination of the EGFR TKI osimertinib and SHP099 strongly suppressed p-MEK and p-ERK, even after 24 h (Fig. 2, right). These

data imply that TKIs in combination with the SHP2 inhibitor SHP099 strongly suppressed the ERK pathway. RAS activity in *ALK*/*ROS1*/*EGFR*-altered cells was also determined, using a RAS-GTP assay (Supplementary Fig. 2B). Consistent with MEK and ERK, RAS activity was not completely inhibited by an oncogene-targeted TKI when used alone. A similar investigation of the AKT pathway showed that SHP099 reduced the level of p-AKT to varying extents in most of the investigated cell lines except ABC-19. However, SHP099 in combination with a TKI showed stronger inhibition of p-AKT (Fig. 2).

The SHP2 inhibitor SHP099 reduces residual cells associated with TKIs

The ability of the SHP2 inhibitor SHP099 to prevent residual cells was also assessed. Oncogene-driven cancer cells were treated with the corresponding TKI with or without SHP099 for 6 days, followed by crystal violet staining to determine the extent of cell proliferation (Fig. 3A). In *ALK*-rearranged H3122 and ABC-19 cells, SHP099 monotherapy resulted in little growth inhibition, whereas alectinib monotherapy significantly inhibited growth but with residual cells after treatment. The combination of SHP099 and alectinib effectively inhibited cell growth, with fewer residual cells remaining than obtained with either monotherapy (Fig. 3A, left). Similarly, SHP099

combined with crizotinib effectively inhibited *ROS1*-rearranged cancer cells (Fig. 3A, center), as also observed with SHP099 combined with osimertinib in *EGFR*-mutant cancer cells (Fig. 3A, right). Based on the proportion of stained cells, addition of SHP099 to the TKI treatment significantly inhibited residual proliferating cells of *ALK/ROS1/EGFR*-altered NSCLC (Fig. 3B).

To determine whether the activity of SHP099 was synergistic or additive, a cell proliferation assay was performed to obtain the CI (Fig. 4). Each TKI, i.e., alectinib for ALK (Fig. 4A, left), crizotinib or DS-6051b for ROS1 (Fig. 4A, center and Supplementary Fig. 2C) or osimertinib for EGFR (Fig. 4A, right), effectively inhibited cell proliferation, whereas SHP099 alone had little effect, with a 50% inhibitory concentration (IC_{50}) > 10 μM in all of the examined cell lines. However, SHP099 shifted the viability curve of cells treated with alectinib, crizotinib/DS-6051b or osimertinib to the left, indicative of a decreased IC_{50} for these drugs in *ALK/ROS1/EGFR*-altered cells. In addition, combined use of SHP099 (1 or 5 μM) with alectinib, crizotinib or osimertinib suppressed cell proliferation to a significantly greater extent than any of the agents alone (Supplementary Fig. 3). The CI was < 1 in the fraction affected (Fa), with a range ≥ 0.5 in all cell lines tested (Fig. 4B), suggesting that the TKIs and SHP099 have synergistic effects in these cell lines.

To confirm that SHP099 acted by inhibiting SHP2 and not through an off-target effect, SHP2 was genetically disrupted using siPTPN11. Because siPTPN11 did not sufficiently inhibit SHP2 expression in the investigated cells (Supplementary Fig. 4), we used another SHP2 inhibitor RMC4550 (33) (Supplementary Fig. 5). Consistent with SHP099, RMC-4550 enhanced the effects of the TKIs in the investigated cell lines; specifically, combined use of RMC-4550 and a TKI yielded greater inhibition of p-ERK and p-AKT than achieved with the TKI alone (Supplementary Fig. 5A) and significantly suppressed cell proliferation (Supplementary Fig. 5B). This result supports the finding that the effects of SHP099 were mediated by SHP2 inhibition, not an off-target activity.

SHP099 enhances the effects of TKIs on xenograft tumors

To examine the combined effects of SHP099 and TKIs *in vivo*, xenograft models were prepared using BALB/c-nu/nu mice. Xenografted tumors derived from *ALK*-rearranged H3122 were treated with vehicle, SHP099, alectinib or a combination of SHP099 and alectinib (Fig. 5). Consistent with the *in vitro* results (Figs. 3, 4A), SHP099 alone had little effect on tumor growth, SHP099 plus alectinib resulted in significantly greater inhibition of the tumors than SHP099 or alectinib alone, but only the two agents used in combination decreased the size of the tumors (Fig. 5). The experiment was then

repeated using xenografted tumors derived from *ROS1*-rearranged ABC-20 cells treated with vehicle, SHP099, crizotinib or their combination. Tumor volume was significantly smaller after combination therapy than after SHP099 or crizotinib monotherapy (Fig. 5). Finally, xenograft tumors derived from *EGFR*-mutant PC-9 cells were treated with vehicle, SHP099, osimertinib or their combination. Tumor growth was more strongly inhibited by the combination therapy than with either monotherapy (Fig. 5). Increased toxicity was not observed with the combination therapy in any of the xenograft models (Supplementary Fig. 6).

SHP099 is comparable to or more effective than MEK inhibitor in enhancing the efficacy of TKIs

In *EGFR*-mutant NSCLC, inhibitors of MEK, a protein downstream of SHP2, enhance the effects of EGFR TKIs by increasing the inhibition of ERK activity (18). To compare the inhibitory effect of SHP2 and MEK inhibitors on residual cells, *EGFR*-mutant NSCLC cells were treated with SHP099 or the MEK inhibitor selumetinib. Either agent, when combined with osimertinib, resulted in more potent inhibition of ERK activity than that achieved with osimertinib alone (Fig. 6A). However, while AKT activity was strongly suppressed by the combination of SHP099 and osimertinib, the combination of

selumetinib and osimertinib was not better than osimertinib alone (Fig. 6A). To determine the effect *in vivo*, xenograft tumors derived from PC-9 cells (*EGFR* ex19 deletion) were treated with osimertinib alone, osimertinib plus selumetinib, or osimertinib plus SHP099. The strongest inhibition of tumor growth was obtained with the combination of osimertinib and SHP099 (Fig. 6B). A signaling analysis of the xenograft tumors (Supplementary Fig. 7A) showed that, unlike the *in vitro* results, combination therapy did not result in the further inhibition of ERK in the xenograft tumor. A possible reason for this difference is that residual cells with persisting ERK cell signaling are more tightly concentrated in the xenograft tumors and thus less responsive to combination therapy with SHP2 or selumetinib. A comparison of the effects of SHP099 and selumetinib in *ALK* (H3122) xenograft tumors showed that, as in the *EGFR* mutant tumors, SHP099 was more potent than selumetinib in enhancing the effects of TKI therapy, even after 6 weeks of treatment (Fig. 6C). Similar results were obtained in *ROS1* rearranged ABC-20 xenograft tumors, in which the combination of SHP099 and crizotinib showed the most effective tumor inhibition, although the difference was not significant compared to the combination of selumetinib and crizotinib (Fig. 6D). There was no difference in the body weights of the xenografted mice (Supplementary Fig. 7B-C).

Discussion

This study demonstrated the ability of the allosteric SHP2 inhibitor to enhance the effects of TKIs in a model of treatment-naïve *ALK*/*ROS1*/*EGFR*-rearranged NSCLC.

SHP2 inhibitors have been evaluated mainly for their ability to overcome acquired resistance in oncogene-driven NSCLC, such as *ALK*-rearranged or *EGFR*-mutant NSCLC (34, 35). Standard oncogene-driven NSCLC treatment involves administration of a molecular-targeting agent to overcome acquired resistance. However, that strategy has not been completely successful, in part because tumor heterogeneity leads to the development of multiple resistance mechanisms within a single tumor. Thus, SHP2 is an effective target for overcoming acquired resistance because it mediates the transduction of multiple RTKs to their downstream pathways, such that its inhibition acts on many resistance mechanisms simultaneously. However, some acquired resistance mechanisms, such as the small cell transition or the epithelial-mesenchymal transition, may be difficult to overcome even with an SHP2 inhibitor.

Residual cells that persist following molecular-targeted therapies have recently garnered attention as a potential cause of acquired resistance. Although the precise mechanisms underlying the survival of residual cells under molecular-targeted therapy remain to be elucidated, reactivated ERK after TKI therapy is thought to play a role (17, 18). Our study showed that in *ALK*/*ROS1*/*EGFR*-altered cancer cells, ERK remained

activated or was reactivated even after 48 h of cell exposure to TKIs (Fig. 1B). SHP2 mediates RTK signaling, forms a complex with GRB2 and SOS, converts RAS-GDP to RAS-GTP and activates downstream ERK signaling (43, 44). Based on these key activities, treating *ALK*/*ROS1*/*EGFR*-altered cancer cells with the SHP2 inhibitor SHP099 was expected to inhibit remaining ERK activity in the residual cells under TKI therapy. While neither the SHP2 inhibitor nor TKI alone completely suppressed ERK activity in *ALK*/*ROS1/EGFR*-altered NSCLC cells, this was achieved by their combination. Moreover, combination treatment was effective in inhibiting residual cancer cells both *in vitro* (Figs. 3, 4) and *in vivo* (Fig. 5). Supporting our observations, combination therapy with erlotinib, an older generation EGFR-TKI, and a SHP2 inhibitor led to synergistic inhibition of *EGFR*-mutant cell proliferation *in vitro* (37). Collectively, our findings indicate that SHP2 inhibition combined with molecular targeting agents represent a promising treatment strategy for *ALK*/*ROS1*/*EGFR*-altered NSCLC.

SHP099 acts not only on the ERK pathway but also on the PI3K/AKT pathway (45, 46) and in this study it suppressed AKT phosphorylation in most of the investigated cell lines, especially in *ROS1*-rearranged HCC78 and ABC-20 cells (Fig. 2 and Supplementary Fig. 4). Other studies have reported that SHP099 did not inhibit pAKT

in *EGFR* or *ALK*-altered models (34, 47), which suggests that the impact of an SHP2 inhibitor on AKT differs in different cell lines.

Combination therapy of osimertinib and the MEK inhibitor selumetinib is currently being evaluated in patients with *EGFR*-mutant NSCLC (19). A comparison of the efficacy of SHP099 vs. selumetinib when used in combination with osimertinib in the treatment of *EGFR*-mutant NSCLC showed the superiority of SHP099 (Fig. 6A). Of note, this more potent effect was not limited to *EGFR*-mutant NSCLC but was also observed in *ALK*/*ROS1*-altered NSCLC (Fig. 6C, D). These results imply that combined use of a TKI and an SHP2 inhibitor, rather than an MEK inhibitor, is the better therapeutic strategy.

In conclusion, the results of this study demonstrate that SHP2 plays an important role in maintaining *ALK*- or *ROS1*-altered or *EGFR*-mutant NSCLC cells that remain under TKI treatment, and that targeting SHP2 enhances the actions of TKIs. Thus, combination therapy consisting of a TKI and an allosteric SHP2 inhibitor may be a novel treatment strategy for TKI-naïve *ALK*/*ROS1*/*EGFR*-altered NSCLC.

Conflicts of Interest

EI received honoraria from Chugai Pharmaceutical. EI received additional research funding

from Eli Lilly Japan. KO received a research grant from Boehringer-Ingelheim, Japan. KH received honoraria and research funding from Chugai Pharmaceutical. YM received honoraria from Chugai Pharmaceutical. KK received honoraria from Chugai Pharmaceuticals. All other authors declare no conflicts of interest regarding this study.

Acknowledgements

We are grateful to Hiromi Nakashima and Kyoko Maeda for their technical support.

References

1. Wu YL, Yang JC, Kim DW, Lu S, Zhou J, Seto T, et al. Phase II study of crizotinib in East Asian patients with ROS1-positive advanced non-small-cell lung cancer. J Clin Oncol. 2018;36(14):1405-11.
2. Shaw AT, Ou SH, Bang YJ, Camidge DR, Solomon BJ, Salgia R, et al. Crizotinib in ROS1-rearranged non-small-cell lung cancer. N Engl J Med. 2014;371(21):1963-71.
3. Peters S, Camidge DR, Shaw AT, Gadgeel S, Ahn JS, Kim DW, et al. Alectinib versus crizotinib in untreated ALK-positive non-small-cell lung cancer. N Engl J Med. 2017;377(9):829-38.
4. Solomon BJ, Mok T, Kim DW, Wu YL, Nakagawa K, Mekhail T, et al. First-line crizotinib versus chemotherapy in ALK-positive lung cancer. N Engl J Med. 2014;371(23):2167-77.
5. Soria JC, Ohe Y, Vansteenkiste J, Reungwetwattana T, Chewaskulyong B, Lee KH, et al. Osimertinib in untreated EGFR-mutated advanced non-small-cell lung cancer. N Engl J Med. 2018;378(2):113-25.
6. Zhou C, Wu YL, Chen G, Feng J, Liu XQ, Wang C, et al. Erlotinib versus chemotherapy as first-line treatment for patients with advanced EGFR mutation-positive non-small-cell lung cancer (OPTIMAL, CTONG-0802): a multicentre, open-label, randomised, phase 3 study. Lancet Oncol. 2011;12(8):735-42.
7. Pao W, Miller VA, Politi KA, Riely GJ, Somwar R, Zakowski MF, et al. Acquired resistance of lung adenocarcinomas to gefitinib or erlotinib is associated with a second mutation in the EGFR kinase domain. PLoS Med. 2005;2(3):e73.
8. Engelman JA, Zejnullahu K, Mitsudomi T, Song Y, Hyland C, Park JO, et al. MET amplification leads to gefitinib resistance in lung cancer by activating ERBB3 signaling. Science. 2007;316(5827):1039-43.
9. Ohashi K, Sequist LV, Arcila ME, Moran T, Chmielecki J, Lin YL, et al. Lung cancers with acquired resistance to EGFR inhibitors occasionally harbor BRAF gene mutations but lack mutations in KRAS, NRAS, or MEK1. Proc Natl Acad Sci U S A. 2012;109(31):E2127-33.
10. Gainor JF, Dardaei L, Yoda S, Friboulet L, Leshchiner I, Katayama R, et al. Molecular mechanisms of resistance to first- and second-generation ALK inhibitors in ALK-rearranged lung cancer. Cancer Discov. 2016;6(10):1118-33.
11. Isozaki H, Ichihara E, Takigawa N, Ohashi K, Ochi N, Yasugi M, et al. Non-small cell lung cancer cells acquire resistance to the ALK inhibitor alectinib by activating alternative receptor tyrosine kinases. Cancer Res. 2016;76(6):1506-16.
12. Mok TS, Wu YL, Ahn MJ, Garassino MC, Kim HR, Ramalingam SS, et al. Osimertinib

431 or platinum-pemetrexed in EGFR T790M-positive lung cancer. N Engl J Med.
432 2017;376(7):629-40.
433 13. Kobayashi S, Boggon TJ, Dayaram T, Jänne PA, Kocher O, Meyerson M, et al. EGFR
434 mutation and resistance of non-small-cell lung cancer to gefitinib. N Engl J Med.
435 2005;352(8):786-92.
436 14. Ou SH, Ahn JS, De Petris L, Govindan R, Yang JC, Hughes B, et al. Alectinib in
437 crizotinib-refractory ALK-rearranged non-small-cell lung cancer: A phase II global study.
438 J Clin Oncol. 2016;34(7):661-8.
439 15. Okada K, Araki M, Sakashita T, Ma B, Kanada R, Yanagitani N, et al. Prediction
440 of ALK mutations mediating ALK-TKIs resistance and drug re-purposing to overcome the
441 resistance. EBioMedicine. 2019;41:105-19.
442 16. Katayama R, Gong B, Togashi N, Miyamoto M, Kiga M, Iwasaki S, et al. The
443 new-generation selective ROS1/NTRK inhibitor DS-6051b overcomes crizotinib resistant
444 ROS1-G2032R mutation in preclinical models. Nat Commun. 2019;10(1):3604.
445 17. Ichihara E, Westover D, Meador CB, Yan Y, Bauer JA, Lu P, et al. SFK/FAK Signaling
446 attenuates osimertinib efficacy in both drug-sensitive and drug-resistant models of
447 EGFR-mutant lung cancer. Cancer Res. 2017;77(11):2990-3000.
448 18. Tricker EM, Xu C, Uddin S, Capelletti M, Ercan D, Ogino A, et al. Combined EGFR/MEK
449 inhibition prevents the emergence of resistance in EGFR-mutant lung cancer. Cancer Discov.
450 2015;5(9):960-71.
451 19. Oxnard GR, Yang JC, Yu H, Kim SW, Saka H, Horn L, et al. TATTON: a multi-arm,
452 phase Ib trial of osimertinib combined with selumetinib, savolitinib, or durvalumab in
453 EGFR-mutant lung cancer. Ann Oncol. 2020;31(4):507-16.
454 20. Tartaglia M, Mehler EL, Goldberg R, Zampino G, Brunner HG, Kremer H, et al.
455 Mutations in PTPN11, encoding the protein tyrosine phosphatase SHP-2, cause Noonan
456 syndrome. Nat Genet. 2001;29(4):465-8.
457 21. Loh ML, Vattikuti S, Schubbert S, Reynolds MG, Carlson E, Lieuw KH, et al.
458 Mutations in PTPN11 implicate the SHP-2 phosphatase in leukemogenesis. Blood.
459 2004;103(6):2325-31.
460 22. Han T, Xiang DM, Sun W, Liu N, Sun HL, Wen W, et al. PTPN11/Shp2 overexpression
461 enhances liver cancer progression and predicts poor prognosis of patients. J Hepatol.
462 2015;63(3):651-60.
463 23. Tartaglia M, Niemeyer CM, Fragale A, Song X, Buechner J, Jung A, et al. Somatic
464 mutations in PTPN11 in juvenile myelomonocytic leukemia, myelodysplastic syndromes and
465 acute myeloid leukemia. Nat Genet. 2003;34(2):148-50.
466 24. Cai P, Guo W, Yuan H, Li Q, Wang W, Sun Y, et al. Expression and clinical

467 significance of tyrosine phosphatase SHP-2 in colon cancer. Biomed Pharmacother.
468 2014;68(3):285-90.
469 25. Aceto N, Sausgruber N, Brinkhaus H, Gaidatzis D, Martiny-Baron G, Mazzarol G,
470 et al. Tyrosine phosphatase SHP2 promotes breast cancer progression and maintains
471 tumor-initiating cells via activation of key transcription factors and a positive feedback
472 signaling loop. Nat Med. 2012;18(4):529-37.
473 26. Zhang RY, Yu ZH, Zeng L, Zhang S, Bai Y, Miao J, et al. SHP2 phosphatase as a
474 novel therapeutic target for melanoma treatment. Oncotarget. 2016;7(45):73817-29.
475 27. Tang C, Luo D, Yang H, Wang Q, Zhang R, Liu G, et al. Expression of SHP2 and related
476 markers in non-small cell lung cancer: a tissue microarray study of 80 cases. Appl
477 Immunohistochem Mol Morphol. 2013;21(5):386-94.
478 28. Mainardi S, Mulero-Sánchez A, Prahallad A, Germano G, Bosma A, Krimpenfort P,
479 et al. SHP2 is required for growth of KRAS-mutant non-small-cell lung cancer in vivo. Nat
480 Med. 2018;24(7):961-7.
481 29. Ahmed TA, Adamopoulos C, Karoulia Z, Wu X, Sachidanandam R, Aaronson SA, et al.
482 SHP2 drives adaptive resistance to ERK signaling inhibition in molecularly defined subsets
483 of ERK-dependent tumors. Cell Rep. 2019;26(1):65-78.e5.
484 30. Wang J, Pollard K, Allen AN, Tomar T, Pijnenburg D, Yao Z, et al. Combined
485 inhibition of SHP2 and MEK is effective in models of NF1-deficient malignant peripheral
486 nerve sheath tumors. Cancer Res. 2020;80(23):5367-79.
487 31. Valencia-Sama I, Ladumor Y, Kee L, Adderley T, Christopher G, Robinson CM, et
488 al. NRAS status determines sensitivity to SHP2 inhibitor combination therapies targeting
489 the RAS-MAPK pathway in neuroblastoma. Cancer Res. 2020;80(16):3413-23.
490 32. Lu H, Liu C, Velazquez R, Wang H, Dunkl LM, Kazic-Legueux M, et al. SHP2 inhibition
491 overcomes RTK-mediated pathway reactivation in KRAS-mutant tumors treated with MEK
492 inhibitors. Mol Cancer Ther. 2019;18(7):1323-34.
493 33. Nichols RJ, Haderk F, Stahlhut C, Schulze CJ, Hemmati G, Wildes D, et al. RAS
494 nucleotide cycling underlies the SHP2 phosphatase dependence of mutant BRAF-, NF1- and
495 RAS-driven cancers. Nat Cell Biol. 2018;20(9):1064-73.
496 34. Dardaei L, Wang HQ, Singh M, Fordjour P, Shaw KX, Yoda S, et al. SHP2 inhibition
497 restores sensitivity in ALK-rearranged non-small-cell lung cancer resistant to ALK
498 inhibitors. Nat Med. 2018;24(4):512-7.
499 35. Sun Y, Meyers BA, Czako B, Leonard P, Mseeh F, Harris AL, et al. Allosteric SHP2
500 inhibitor, IACS-13909, overcomes EGFR-dependent and EGFR-independent resistance
501 mechanisms toward osimertinib. Cancer Res. 2020;80(21):4840-53.
502 36. Liu C, Lu H, Wang H, Loo A, Zhang X, Yang G, et al. Combinations with allosteric

503 SHP2 inhibitor TNO155 to block receptor tyrosine kinase signaling. Clin Cancer Res.
504 2021;27(1):342-54.
505 37. Ito M, Codony-Servat J, Giménez-Capitán A, Serra-Mitjans M, Pérez-Ochoa F, Llige
506 D, et al. Src-homology 2 domain-containing phosphatase 2 in resected EGFR
507 mutation-positive lung adenocarcinoma. JTO Clinical and Research Reports.
508 2020;1(4):100084.
509 38. Kato Y, Ninomiya K, Ohashi K, Tomida S, Makimoto G, Watanabe H, et al. Combined
510 effect of cabozantinib and gefitinib in crizotinib-resistant lung tumors harboring ROS1
511 fusions. Cancer Sci. 2018;109(10):3149-58.
512 39. Mosmann T. Rapid colorimetric assay for cellular growth and survival: application
513 to proliferation and cytotoxicity assays. J Immunol Methods. 1983;65(1-2):55-63.
514 40. Chang TT, Chou TC. Rational approach to the clinical protocol design for drug
515 combinations: a review. Acta Paediatr Taiwan. 2000;41(6):294-302.
516 41. Chou TC, Talaly P. A simple generalized equation for the analysis of multiple
517 inhibitions of Michaelis-Menten kinetic systems. J Biol Chem. 1977;252(18):6438-42.
518 42. Chou TC. Drug combination studies and their synergy quantification using the
519 Chou-Talalay method. Cancer Res. 2010;70(2):440-6.
520 43. Shi ZQ, Yu DH, Park M, Marshall M, Feng GS. Molecular mechanism for the Shp-2
521 tyrosine phosphatase function in promoting growth factor stimulation of Erk activity. Mol
522 Cell Biol. 2000;20(5):1526-36.
523 44. Dance M, Montagner A, Salles JP, Yart A, Raynal P. The molecular functions of
524 Shp2 in the Ras/Mitogen-activated protein kinase (ERK1/2) pathway. Cell Signal.
525 2008;20(3):453-9.
526 45. Ivins Zito C, Kontaridis MI, Fornaro M, Feng GS, Bennett AM. SHP-2 regulates the
527 phosphatidylinositide 3'-kinase/Akt pathway and suppresses caspase 3-mediated apoptosis.
528 J Cell Physiol. 2004;199(2):227-36.
529 46. Tang C, Luo H, Luo D, Yang H, Zhou X. Src homology phosphotyrosyl phosphatase
530 2 mediates cisplatin-related drug resistance by inhibiting apoptosis and activating the
531 Ras/PI3K/Akt1/survivin pathway in lung cancer cells. Oncol Rep. 2018;39(2):611-8.
532 47. Chen YN, LaMarche MJ, Chan HM, Fekkes P, Garcia-Fortanet J, Acker MG, et al.
533 Allosteric inhibition of SHP2 phosphatase inhibits cancers driven by receptor tyrosine
534 kinases. Nature. 2016;535(7610):148-52.

535

536

Figure Legends

Figure 1. Residual cells of *ALK/ROS1/EGFR*-altered NSCLC following TKI therapy.

(A) The cells were treated for 48 h with DMSO or a TKI. H3122 cells were treated with alectinib (Alec, 1 μM), HCC78 cells with crizotinib (Cri, 5 μM) and PC-9 cells with osimertinib (Osi, 1 μM). (B) Immunoblots of the indicated proteins in H3122 and ABC-19 cells treated with DMSO for 4 h or with alectinib (100 nM) for 4, 24 or 72 h; HCC78 and ABC-20 cells treated with DMSO for 4 h or crizotinib (1 μM) for 4, 24 or 72 h and PC-9 and HCC827 cells treated with DMSO for 4 h or osimertinib (100 nM) for 4, 24 or 72 h.

Figure 2. Inhibition of ERK and AKT activities by SHP099 combined with a TKI. Immunoblots of the indicated proteins in H3122 and ABC-19 cells treated with alectinib (Alec, 100 nM), HCC78 and ABC-20 cells treated with crizotinib (Cri, 1 μM) and PC-9 and HCC827 cells treated with osimertinib (Osi, 100 nM) for 24 h. All cell lines were also treated with SHP099 (SHP, 5 μM) for 24 h. Comb, combination.

Figure 3. Inhibition of cancer cell proliferation by SHP099 combined with a TKI.

(A) Crystal-violet-stained cells after drug loading for 6 days. Cancer cells were treated with 1 or 5 μM SHP099 combined with 100 nM alectinib (H3122 and ABC-19), 1 μM crizotinib (HCC78 and ABC-20) or 100 nM osimertinib (PC-9 and HCC827) for 6 days. Alec, alectinib; Cri, crizotinib; Osi, osimertinib. (B) The crystal-violet-stained cells were quantified (n=3). Error bars represent the standard error. *P < 0.01 (one-way ANOVA and Bonferroni method). S, SHP099; A, alectinib; C, crizotinib; O, osimertinib.

Figure 4. Enhanced effect of SHP099 on cell viability inhibition by TKIs *in vitro*. (A) Cell viability curves for cell lines treated with the molecular-targeted drug alone (circles), SHP099 alone (triangles) or the molecular-targeted drug and SHP099 (5 μM) (squares). All drugs were loaded for 96 h. Error bars represent the standard error. SHP, SHP099; Alec, alectinib; Cri, crizotinib; Osi, osimertinib. (B) In the *ALK*-rearranged cell lines (H3122 and ABC-19), the ratio of the alectinib and SHP099 concentrations was 1:50. In the *ROS1*-rearranged cell lines (HCC78 and ABC-20), the ratio of the crizotinib and SHP099 concentrations was 1:5. In the *EGFR*-mutant cell lines (PC-9 and HCC827 cells), the ratio of the osimertinib and SHP099 concentrations was 1:50. CI, combination index; Fa, fraction affected.

Figure 5. Combination of a TKI and an SHP2 inhibitor in a xenograft mouse model. Mice transplanted with H3122, ABC-20 or PC-9 cells were orally administered TKIs and SHP099 (50 mg/kg/day) five times weekly. Mice bearing H3122 tumors were treated with vehicle, alectinib (10 mg/kg/day), SHP099 or alectinib plus SHP099. Mice bearing ABC-20 tumors were treated with vehicle, crizotinib (50 mg/kg/day), SHP099 or crizotinib plus SHP099. Mice bearing PC-9 tumors were treated with vehicle, osimertinib (5 mg/kg/day), SHP099 or osimertinib plus SHP099. Error bars represent the standard error. *P < 0.01 (Student's *t*-test).

Figure 6. Comparison of the effects of SHP099 vs. selumetinib. (A) Immunoblots of the indicated proteins in PC-9 cells treated for 24 h with osimertinib (Osi, 100 nM), selumetinib (Selu, 500 nM) or SHP099 (SHP, 5 μM). p-AKT was quantified using ImageJ software. (B) Mice bearing PC-9 tumors were treated with osimertinib (5 mg/kg/day), osimertinib plus selumetinib (50 mg/kg/day) or osimertinib plus SHP099 (50 mg/kg/day). (C) Mice bearing H3122 tumors were treated with alectinib (10 mg/kg/day), alectinib plus selumetinib (50 mg/kg/day) or alectinib plus SHP099 (50 mg/kg/day). (D) Mice bearing ABC-20 tumors were treated with crizotinib (50

mg/kg/day), crizotinib plus selumetinib (50 mg/kg/day) or crizotinib plus SHP099 (50 mg/kg/day). All drugs were orally administered five times weekly. Error bars represent the standard error. *P < 0.05 (Student's *t*-test).

Figure 1

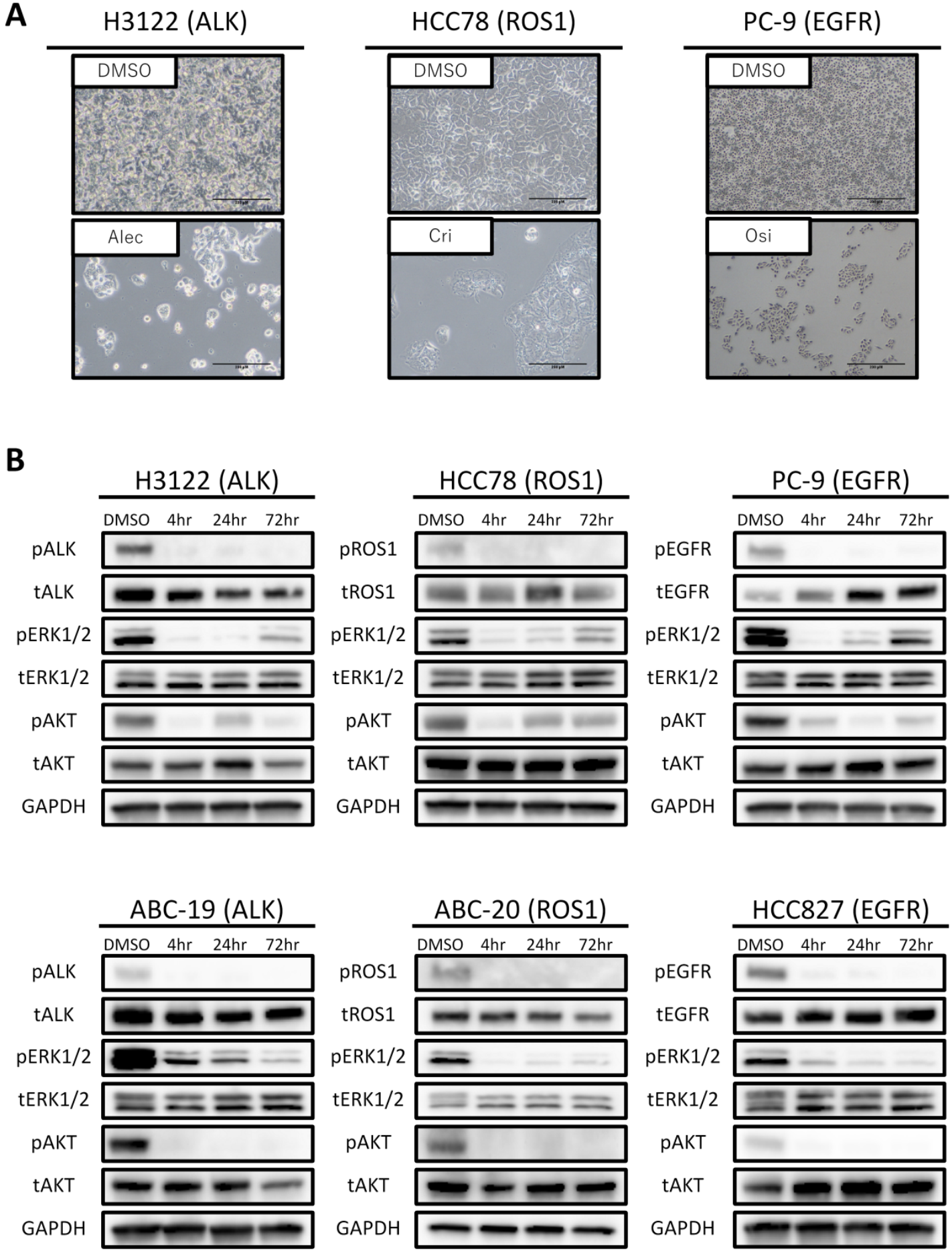
A
H3122 (ALK)
HCC78 (ROS1)
PC-9 (EGFR)
DMSO
DMSO
DMSO
Alec
Cri
Osi
B
H3122 (ALK)
HCC78 (ROS1)
PC-9 (EGFR)
DMSO 4hr 24hr 72hr
pALK
tALK
pERK1/2
tERK1/2
pAKT
tAKT
GAPDH
pROS1
tROS1
pEGFR
tEGFR
ABC-19 (ALK)
ABC-20 (ROS1)
HCC827 (EGFR)

Figure 2

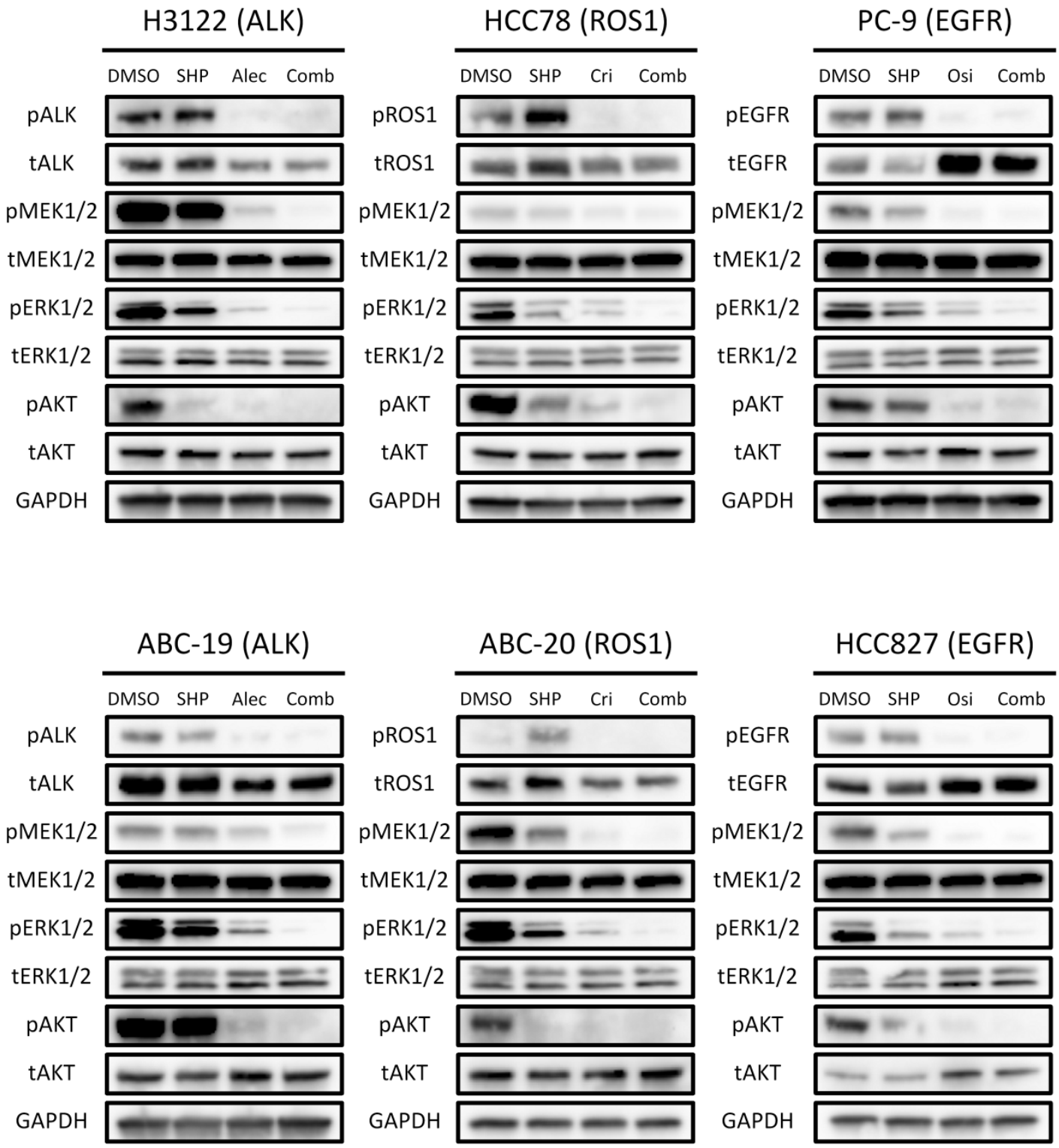
H3122 (ALK)
DMSO SHP Alec Comb
pALK
tALK
pMEK1/2
tMEK1/2
pERK1/2
tERK1/2
pAKT
tAKT
GAPDH
HCC78 (ROS1)
DMSO SHP Cri Comb
pROS1
tROS1
pMEK1/2
tMEK1/2
pERK1/2
tERK1/2
pAKT
tAKT
GAPDH
PC-9 (EGFR)
DMSO SHP Osi Comb
pEGFR
tEGFR
pMEK1/2
tMEK1/2
pERK1/2
tERK1/2
pAKT
tAKT
GAPDH
ABC-19 (ALK)
DMSO SHP Alec Comb
pALK
tALK
pMEK1/2
tMEK1/2
pERK1/2
tERK1/2
pAKT
tAKT
GAPDH
ABC-20 (ROS1)
DMSO SHP Cri Comb
pROS1
tROS1
pMEK1/2
tMEK1/2
pERK1/2
tERK1/2
pAKT
tAKT
GAPDH
HCC827 (EGFR)
DMSO SHP Osi Comb
pEGFR
tEGFR
pMEK1/2
tMEK1/2
pERK1/2
tERK1/2
pAKT
tAKT
GAPDH

Figure 3

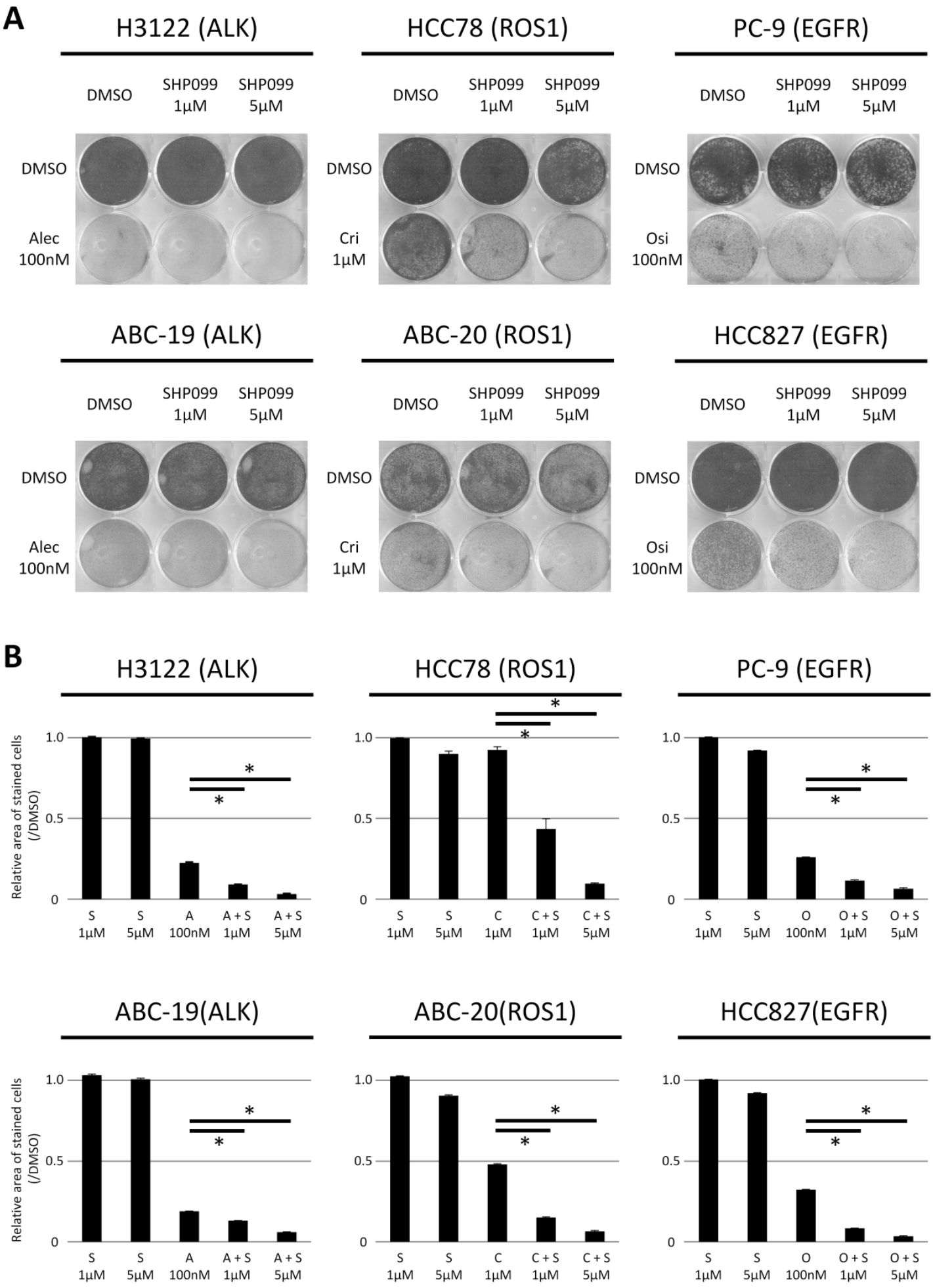
A
H3122 (ALK)
HCC78 (ROS1)
PC-9 (EGFR)
DMSO
SHP099 1μM
SHP099 5μM
DMSO
Alec 100nM
Cri 1μM
Osi 100nM
ABC-19 (ALK)
ABC-20 (ROS1)
HCC827 (EGFR)
B
Relative area of stained cells (/DMSO)
1.0
0.5
0
S 1μM
S 5μM
A 100nM
A + S 1μM
A + S 5μM
C 1μM
C + S 1μM
C + S 5μM
O 100nM
O + S 1μM
O + S 5μM
*

Figure 4

A

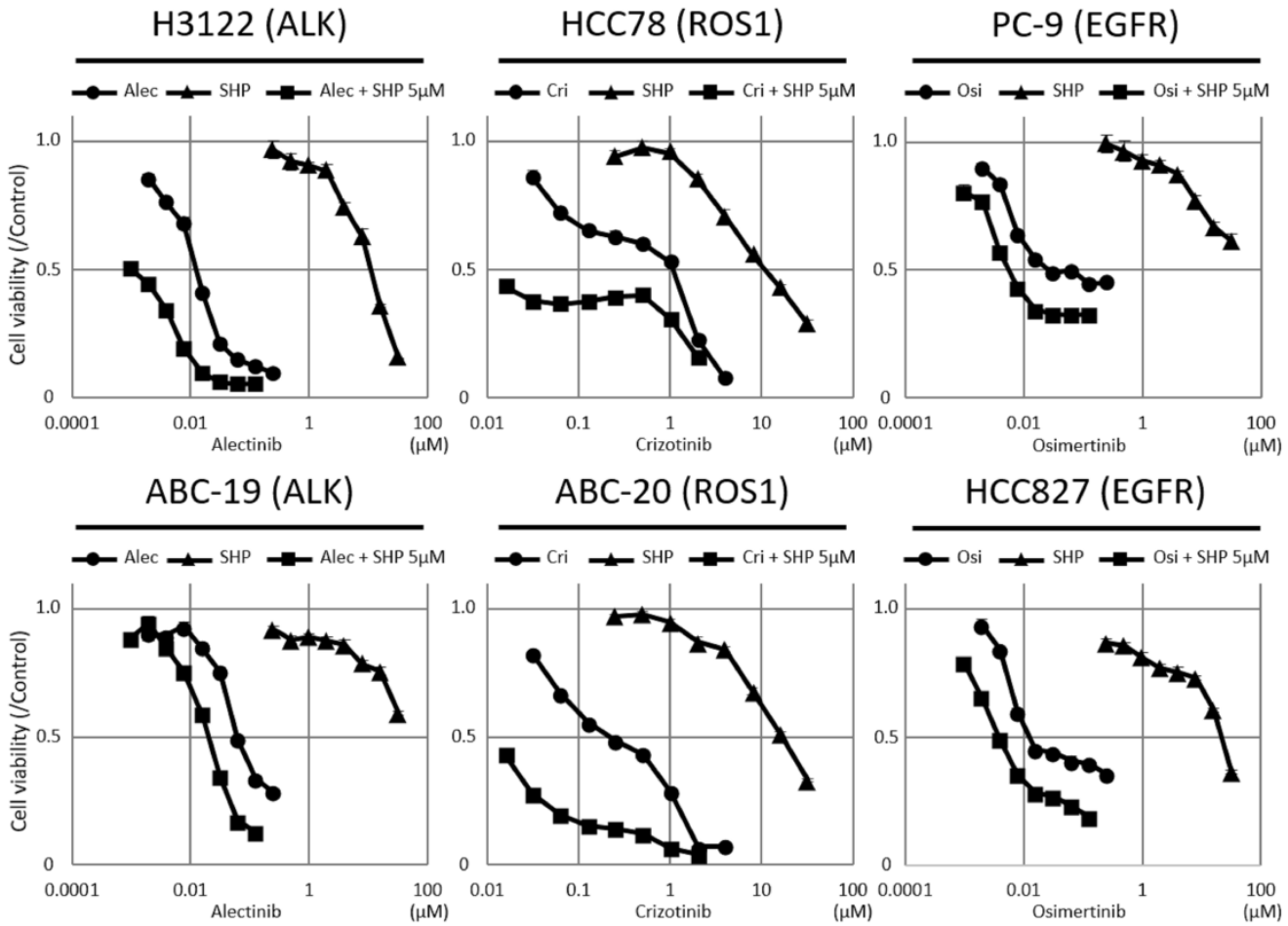
H3122 (ALK)
HCC78 (ROS1)
PC-9 (EGFR)
ABC-19 (ALK)
ABC-20 (ROS1)
HCC827 (EGFR)
Alec
SHP
Alec + SHP 5μM
Cri
Cri + SHP 5μM
Osi
Osi + SHP 5μM
Cell viability (/Control)
1.0
0.5
0
0.0001
0.01
0.1
1
10
100
(μM)
Alectinib
Crizotinib
Osimertinib

B

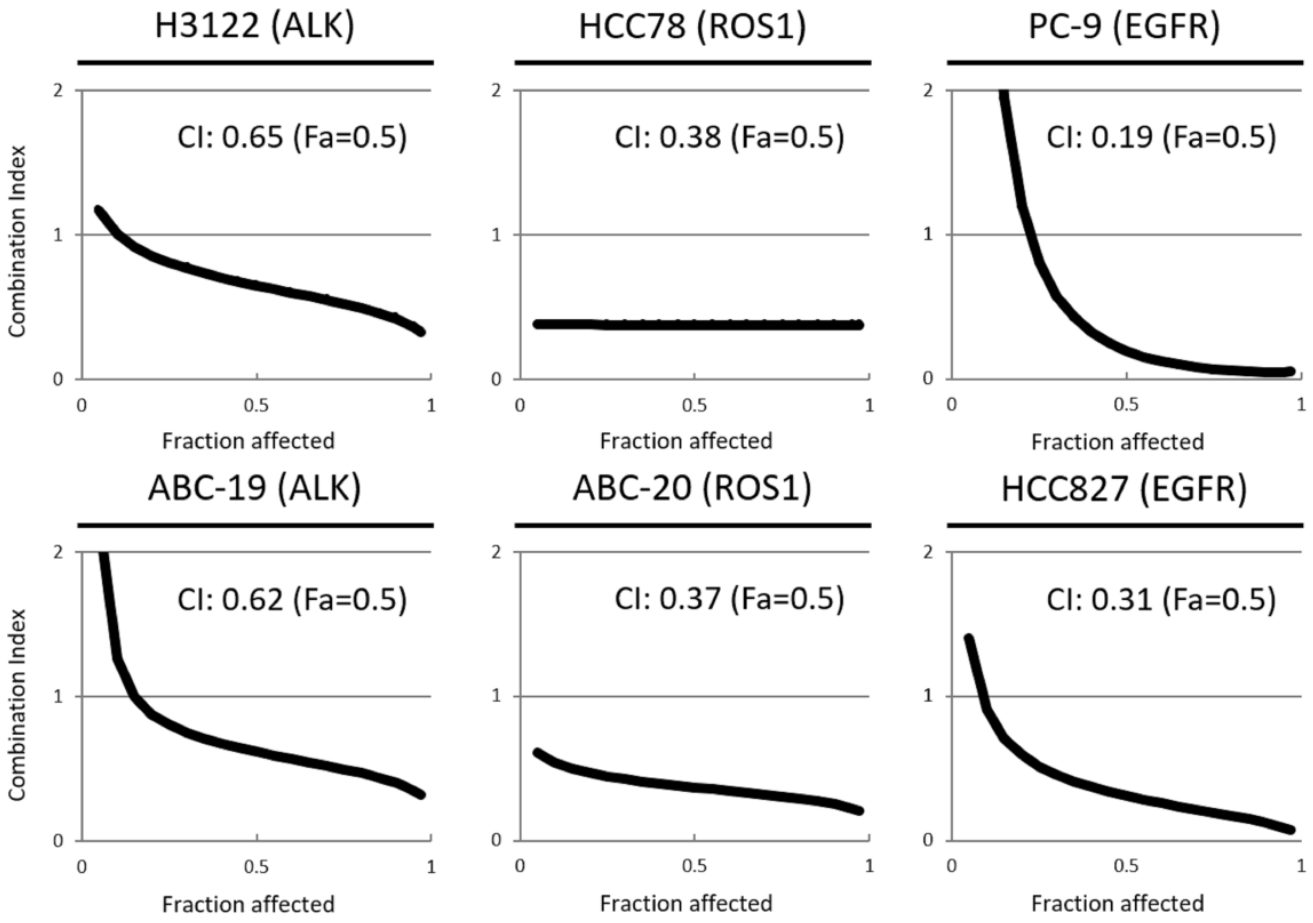
H3122 (ALK)
HCC78 (ROS1)
PC-9 (EGFR)
ABC-19 (ALK)
ABC-20 (ROS1)
HCC827 (EGFR)
CI: 0.65 (Fa=0.5)
CI: 0.38 (Fa=0.5)
CI: 0.19 (Fa=0.5)
CI: 0.62 (Fa=0.5)
CI: 0.37 (Fa=0.5)
CI: 0.31 (Fa=0.5)
Combination Index
Fraction affected
0
0.5
1
2

Figure 5

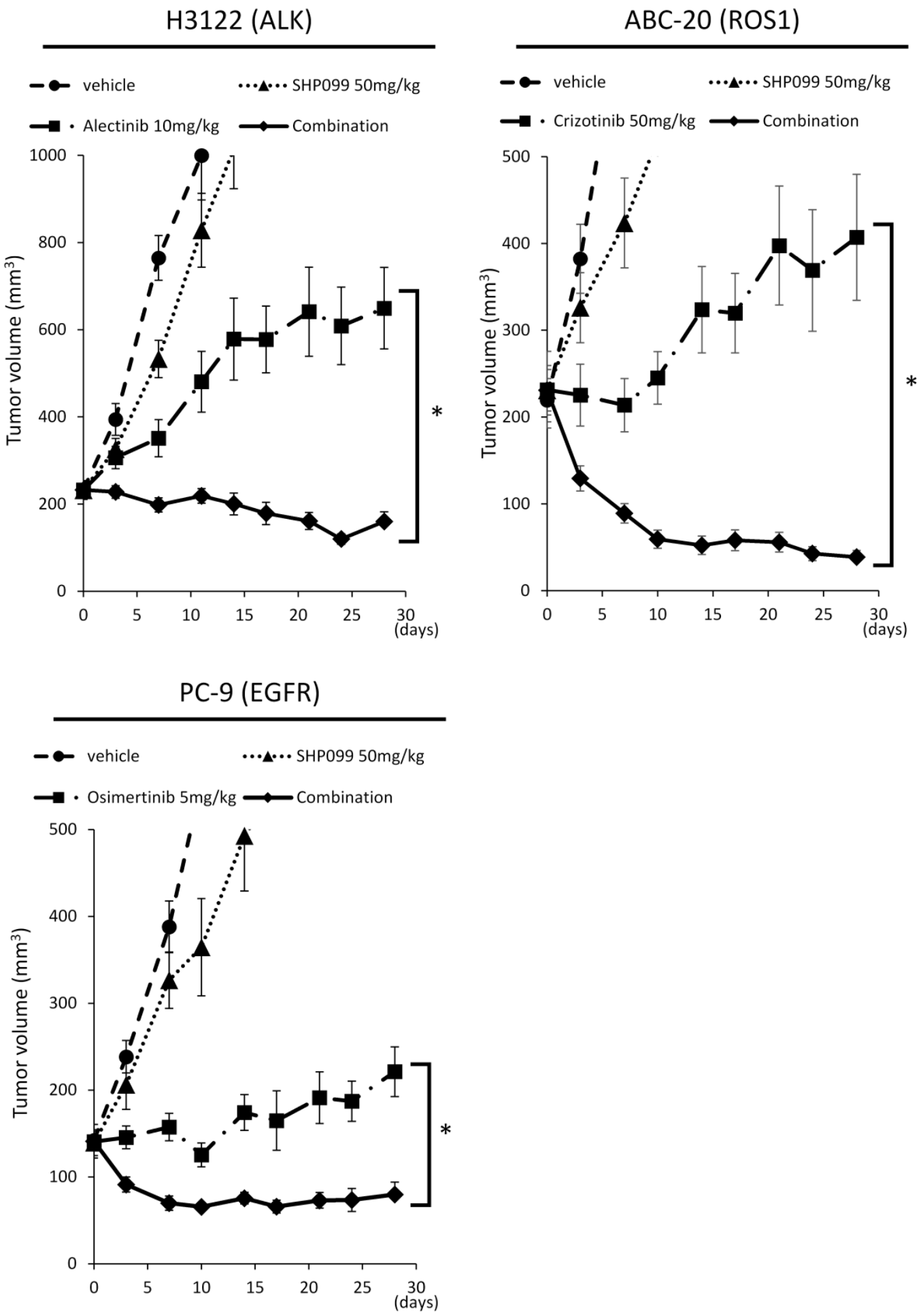
H3122 (ALK)
vehicle
SHP099 50mg/kg
Alectinib 10mg/kg
Combination
Tumor volume (mm3)
(days)
*
ABC-20 (ROS1)
vehicle
SHP099 50mg/kg
Crizotinib 50mg/kg
Combination
Tumor volume (mm3)
(days)
*
PC-9 (EGFR)
vehicle
SHP099 50mg/kg
Osimertinib 5mg/kg
Combination
Tumor volume (mm3)
(days)
*

Figure 6

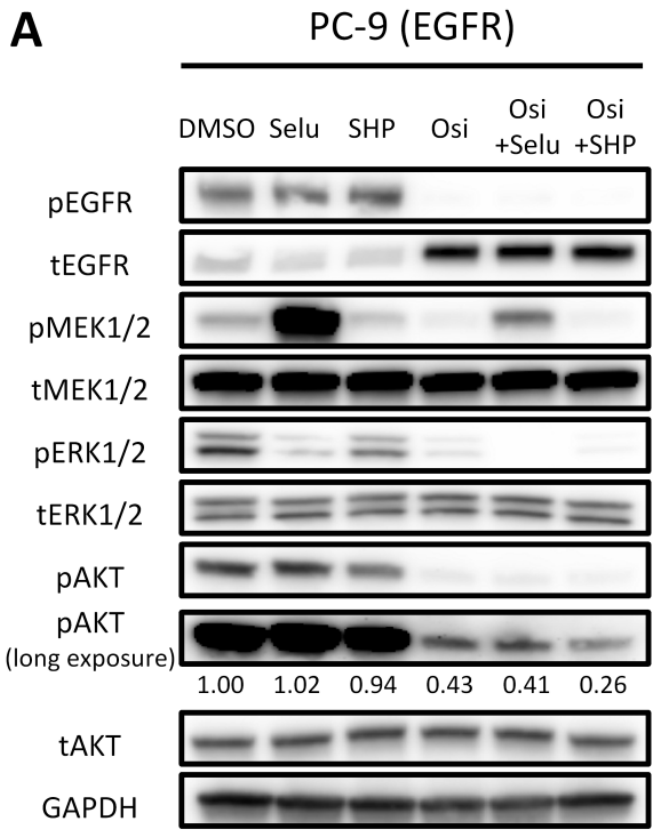
A
PC-9 (EGFR)
DMSO
Selu
SHP
Osi
Osi +Selu
Osi +SHP
pEGFR
tEGFR
pMEK1/2
tMEK1/2
pERK1/2
tERK1/2
pAKT
pAKT (long exposure)
1.00 1.02 0.94 0.43 0.41 0.26
tAKT
GAPDH

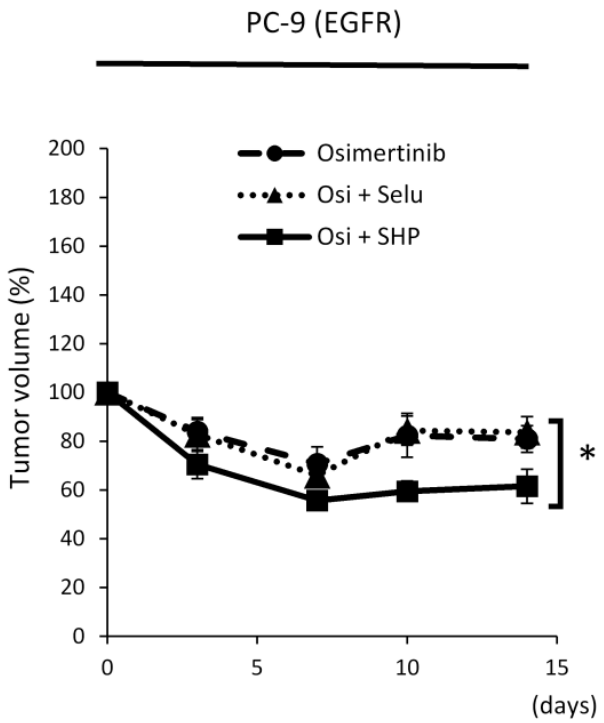
B
PC-9 (EGFR)
Osimertinib
Osi + Selu
Osi + SHP
Tumor volume (%)
(days)
*

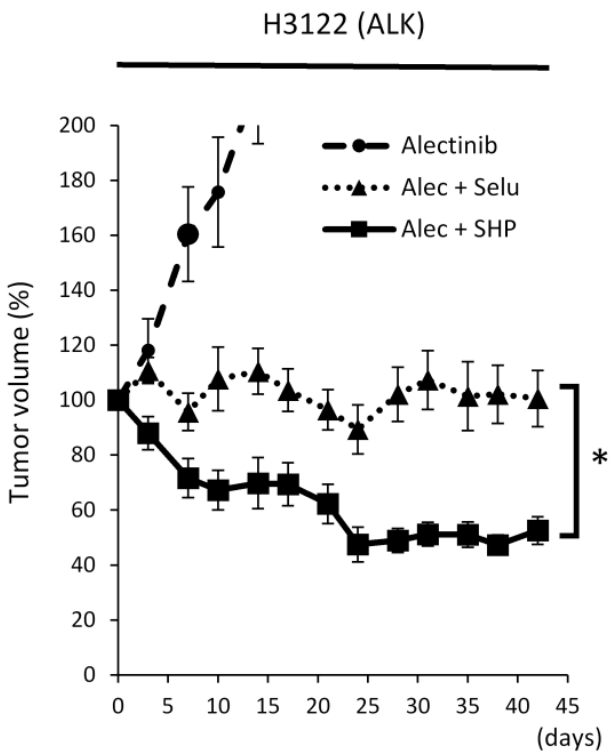
C
H3122 (ALK)
Alectinib
Alec + Selu
Alec + SHP
Tumor volume (%)
(days)
*

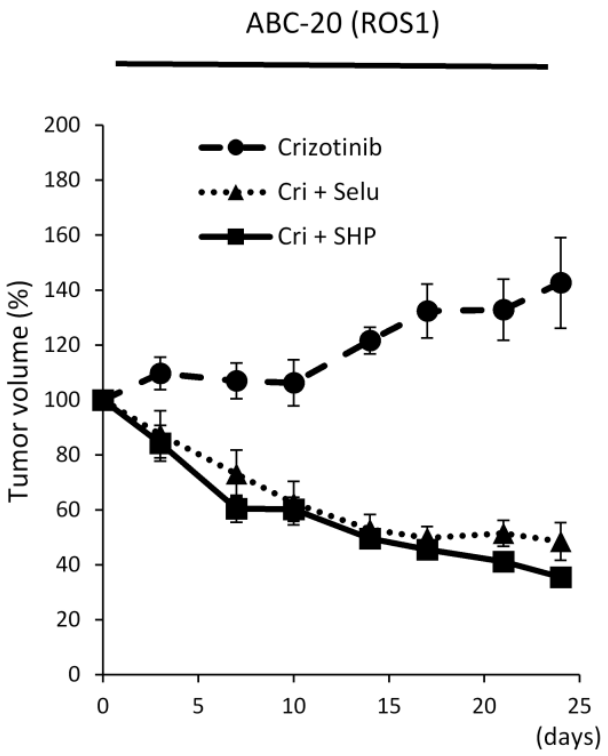
D
ABC-20 (ROS1)
Crizotinib
Cri + Selu
Cri + SHP
Tumor volume (%)
(days)